American Mineralogist, Volume 71, pages 1–16, 1986

Feldspar solid solutions

HERBERT KROLL, ILSE SCHMIEMANN AND GISELA VON CÖLLN

Institut für Mineralogie, Westfälische Wilhelms-Universität
Corrensstr. 24, D-4400 Münster, West Germany

Abstract

Solid solution series of ordered and disordered alkali and ternary feldspars were prepared to provide reference data to estimate structural state and chemical composition and to characterize feldspar volume behavior. Indexing charts based on those powder diffraction lines that were actually used in refining lattice parameters are given as a practical guide in indexing analbite (AA)–high sanidine (HS) and low albite (LA)–low microcline (LM) solid solutions. The triclinic/monoclinic transformation in the AA–HS series is found to occur at 34 mol% Or. Mole fraction Or (n_{Or}) is related to cell volume (V) by equations for the (AA)–(HS) series,

$$n_{Or} = -535.186 + 2.37332V - 3.52656\cdot10^{-3}V^2 + 1.75614\cdot10^{-6}V^3$$
$$\text{s.e.e.} = 0.003n_{Or} \text{ (s.e.e. = standard error of estimate),}$$

and the (LA)–(LM) series,

$$n_{Or} = -1209.142 + 5.28104V - 7.70522\cdot10^{-3}V^2 + 3.75650\cdot10^{-6}V^3$$
$$\text{s.e.e.} = 0.004n_{Or}.$$

The influence of An-content on estimating n_{Or} can be accounted for from the volume data of the ternary series. The volume behavior of the alkali feldspars is characterized by Margules parameters W_V[cal/bar] that are similar for AA and HS:

$$W_{V(AA)} = 0.083(7), \qquad W_{V(HS)} = 0.070(11),$$

but are markedly dissimilar for LA and LM:

$$W_{V(LA)} = 0.111(5), \qquad W_{V(LM)} = 0.015(12).$$

That is, the excess volume is nearly symmetric in the disordered series, but it is definitely asymmetric in the ordered series and thus depends on the degree of Al,Si order. Its behavior is discussed in terms of two factors: geometrical dilatation and chemical contraction.

Introduction

Estimation of the Al,Si distribution in feldspars from their lattice parameters has become routine. The proposed determinative diagrams and equations use as their frame of reference crystal structure analyses and solid solution series of constant and known Al,Si distribution. Kroll (1983) and Kroll and Ribbe (in prep.) review and modify the determinative methods on the basis of recent structure refinements and of several solid solution series which were prepared for this purpose. These series also serve as references for estimating Or-content and for interpreting volume behavior which has lastly been discussed by Hovis (1977), Hovis and Peckins (1978) and Newton and Wood (1980). We report results on these topics with regard to the following series: (1) Low albite (LA)–low microcline (LM); (2) Analbite (AA)–high sanidine (HS); (3) Three series of low ternary feldspars $Ab_xOr_yAn_z$, where z = 16.5, 21.5, 27.8, respectively (x + y + z = 100); (4) Two series of high ternary feldspars $Ab_xOr_yAn_z$, where z = 16.5 and 27.0, respectively.

In the following, the term *topochemical symmetry* will be used to characterize Al,Si distribution independent of the actual symmetry of the feldspar. In the sense of Smith (1970) a feldspar is said to be topochemically monoclinic/triclinic, if its Al,Si distribution does/does not allow the feldspar to be monoclinic, e.g., monalbite and analbite are topochemically monoclinic, whereas high and low albite are topochemically triclinic.

Experimental

Low albite–low microcline series

To date, two such solid solution series have been prepared by Orville (1967) and Waldbaum and Robie (1971), and Hovis and Peckins (1978) have re-refined the Waldbaum and Robie cell parameters. Both of these solid solution series were produced from low microcline by ion-exchange in molten NaCl to give low albite. Mixtures of the end members were then homogenized at elevated temperatures. We found, however, that Na-exchange of low microcline as well as K-exchange of low albite does not produce samples that have the same lattice parameters as have

0003–004X/86/0102–0001$02.00

Table 1. Effect of ion-exchange on low albite and low microcline unit cell parameters

Sample No.	Feldspar	a [Å] 1)	b [Å]	c [Å]	α [°]	β [°]	γ [°]	V [Å^3]	No. lines
6436o	B121 - Low albite	8.1414(12)	12.7881(8)	7.1489(8)	94.201(9)	116.567(6)	87.948(8)	663.91(19)	47
6459m	After K- and Na-exchange	8.1452(26)	12.7877(22)	7.1529(19)	94.181(14)	116.554(15)	87.949(15)	664.66(41)	27
6436m	After K-exchange only	8.5886(7)	12.9636(8)	7.2169(6)	90.576(6)	115.958(5)	87.878(7)	721.95(13)	62
6375m	Cazadero - Low albite	8.1353(7)	12.7852(7)	7.1582(7)	94.274(6)	116.600(5)	87.685(6)	663.86(14)	65
6460o	After K- and Na-exchange	8.1388(12)	12.7870(9)	7.1561(7)	94.246(8)	116.597(6)	87.685(6)	664.08(17)	40
6971m	After K-exchange only	8.5886(6)	12.9621(5)	7.2227(4)	90.633(4)	115.945(3)	87.625(4)	722.39(9)	63
7155m	Prilep - Low microcline	8.5918(7)	12.9612(8)	7.2211(5)	90.623(6)	115.945(4)	87.683(5)	722.48(12)	62
6041	After Na- and K-exchange	8.5895(26)	12.9680(13)	7.2201(19)	90.674(9)	115.979(14)	87.683(9)	722.36(45)	27
6030	After Na-exchange only	8.1372(13)	12.7931(10)	7.1530(9)	90.236(8)	116.617(8)	87.742(7)	663.88(21)	33

1) Standard errors are given in parentheses and refer to the last decimal place(s).

their natural equivalents. In particular, the γ angle is larger by 0.06° in Na-exchanged low microcline than it is in natural low albite, and vice versa for K-exchanged low albite and natural low microcline (Table 1). The difference in γ is not due to a change in the Al,Si distribution produced by the exchange process: if so, the Al,Si order would have decreased during Na-exchange, but increased during K-exchange, which is unlikely; furthermore, after Na-(K-)exchange and K-(Na-)back-exchange the γ angle of the original material is restored, demonstrating that no change of order occurs. Apparently the γ angle is larger in a transformation-twinned low microcline than in a sample lacking this type of twinning, i.e., in a low microcline prepared from low albite.

We therefore decided not to use end members that had been prepared by ion-exchange, but chose natural low microcline (perthitic amazonite) from Prilep, Yugoslavia and low albite from Cazadero, California. Both feldspars are fully ordered as demonstrated by structure refinements (Strob, 1983; Wenk and Kroll, 1984). Tables 2 and 3 give details of their origin, composition and treatment.

The solid solution series was prepared in the following way: Cazadero albite and Prilep microcline were first ground in a ball

Table 2. Preparation of end members for alkali and ternary feldspar series

No.	Original feldspar	Locality	Treatment	Product feldspar	
	Low albite - low microcline series				
1	Low albite	Cazadero, California	none	low albite	Caz
2	Low microcline	Prilep, Yugoslavia	ion-exchanged in KCl: 5h/850°C/1:50*	low microcline	Pri-K
	Analbite - high sanidine series				
3	Low albite	Cazadero, California	annealed at 1090°C, 110d	analbite	Caz-h
4	Analbite Caz-h		ion-exchanged in KCl: 5h/825°C/1:50	high sanidine	Caz-h-k
	Low ternary feldspar series				
5	Low oligoclase (An16.5)	Sultan Hamud, Kenya	none	low oligoclase	84
6	Low oligoclase		ion-exchanged in KCl: 6h/850°C/1:50	low K-oligoclase	
7	Low oligoclase (An21.5)	Arendal, Norway	none	low oligoclase	166
8	Low oligoclase		ion-exchanged in KCl: 6h/850°C/1:50	low K-oligoclase	
9	Low oligoclase (An27.8)	Quebec, Canada	none	low oligoclase	31
10	Low oligoclase		ion-exchanged in KCl: 6h/850°C/1:50	low K-oligoclase	
	High ternary feldspar series				
11	Low oligoclase (An16.5)	Arendal, Norway	annealed at 1090°C,29d + 1110°C,30d	high oligoclase	Vis
12	High oligoclase Vis		ion-exchanged in KCl: 3h/825°C/1:50	high K-oligoclase	
13	Low oligoclase (An27.8)	Quebec, Canada	annealed at 1120°C, 31d	high oligoclase	31h
14	High oligoclase 31h		ion-exchanged in KCl: 7h/900°C/1:60	high K-oligoclase	

* Run duration is given in hours (h) or days (d). Weight proportion feldspar sample : KCl was 1:50 or 1:60 in the exchange experiments.

Table 3. Chemical composition of end member feldspars

No.	End-member feldspar		Composition Ab-Or-An[mol%]			Analyst	
1	Low albite	Caz	99.7	0.2	0.1	H. Rettmar, Münster	(EMP)*
2	Low microcline	Pri-K	0.1	99.8	0.1	D. Maury, Münster	(AAS)*
			(0	99.9	0.1)**		
3	Analbite	Caz-h	99.4	0.3	0.3	A. Bischoff, Münster	(EMP)
4	High sanidine	Caz-h-K	0.9	98.9	0.3	A. Schmidt, Münster	(AAS)
			(0	99.7	0.3)**		
5	Low oligoclase	84	82.8	0.7	16.5	Corlett & Eberhard (1967)	(EMP)
6	Low K-oligoclase		0	83.5	16.5	complete exchange assumed	
7	Low oligoclase	166	77.3	1.2	21.5	Corlett & Eberhard (1967)	(EMP)
8	Low K-oligoclase		0	78.5	21.5	complete exchange assumed	
9	Low oligoclase	31	69.9	2.3	27.8	Corlett & Eberhard (1967)	(EMP)
10	Low K-oligoclase		0	72.2	27.8	complete exchange assumed	
11	High oligoclase	Vis	79.0	4.5	16.5	H. Rettmar, Münster	(EMP)
12	High K-oligoclase		0	83.5	16.5	complete exchange assumed	
13	High oligoclase	31h	67.5	5.5	27.0	I. Schmiemann, Münster	(AAS)
14	High K-oligoclase		0	72.2	27.8	complete exchange assumed	

* EMP = Electron Microprobe, AAS = Atomic Absorption Spectrometry. ** See text.

mill and then in an agate mortar down to a grain size routinely used in X-ray powder photography (<10 μm). Prilep microcline was K-exchanged to remove its non-exsolved Na content and to convert the exsolved (perthitic) albite into low microcline. The amount of perthitic albite in the bulk sample was determined by atomic absorption spectroscopy (AAS) to be 9 mol%. The influence of its K-exchange equivalent on the γ angle of the bulk exchange product can thus be considered negligible. Mixtures of

Table 4. Unit cell parameters of low albite–low microcline solid solutions

Sample No.	Or	Ab	An	Homogenization t[hours]	T[°C]	a [Å]	b [Å]	c [Å]	α [°]	β [°]	γ [°]	V [Å^3]	No. lines
	[mol%]												
6375m	0.2	99.7	0.1	(1)**		8.1355(7)*	12.7853(8)	7.1583(6)	94.278(6)	116.606(5)	87.684(5)	663.84(13)	65
7199o	0.2	99.7	0.1	(1)**	40/900	8.1355(8)	12.7843(6)	7.1580(6)	94.261(5)	116.607(5)	87.693(5)	663.78(13)	73
8423o	5.0	94.9	0.1	(1)**	40/900	8.1599(7)	12.7962(6)	7.1604(7)	94.107(6)	116.539(5)	87.662(5)	667.13(12)	68
7199m	5.0	94.9	0.1	40	900	8.1576(8)	12.7947(6)	7.1611(7)	94.120(6)	116.537(5)	87.664(4)	666.92(15)	55
8423m	10.0	89.9	0.1	40	900	8.1790(11)	12.8082(8)	7.1663(7)	93.959(7)	116.491(6)	87.642(6)	670.25(18)	61
7199u	10.0	89.9	0.1	40	900	8.1783(10)	12.8089(8)	7.1651(8)	93.960(7)	116.487(6)	87.629(6)	670.14(17)	53
8423u	15.0	84.9	0.1	40	900	8.1983(14)	12.8216(7)	7.1700(12)	93.771(9)	116.439(8)	87.635(8)	673.32(25)	43
7207o	15.0	84.9	0.1	40	900	8.1967(13)	12.8214(9)	7.1691(11)	93.766(9)	116.432(8)	87.637(8)	673.14(23)	55
8458o	20.0	79.9	0.1	40	1000	8.2237(12)	12.8328(14)	7.1758(10)	93.550(13)	116.352(8)	87.627(12)	677.21(23)	35
7320o	20.0	79.9	0.1	40/900+20/1000		8.2253(10)	12.8369(8)	7.1746(8)	93.520(9)	116.357(6)	87.605(7)	677.42(17)	58
7320m	25.0	74.9	0.1	40/900+20/1000		8.2482(11)	12.8542(10)	7.1790(8)	93.286(10)	116.286(7)	87.552(10)	681.19(18)	40
7320u	30.0	69.9	0.1	40/900+20/1000		8.2761(12)	12.8692(9)	7.1852(9)	92.971(12)	116.227(8)	87.554(10)	685.40(20)	44
7322o	35.0	64.9	0.1	40/900+20/1000		8.2973(20)	12.8786(12)	7.1896(15)	92.716(14)	116.178(12)	87.564(11)	688.49(35)	40
7322m	40.0	59.9	0.1	40/900+20/1000		8.3228(8)	12.8973(7)	7.1946(7)	92.393(7)	116.134(7)	87.534(6)	692.46(15)	42
7322u	45.0	54.9	0.1	40/900+20/1000		8.3458(11)	12.9100(8)	7.1985(7)	92.075(9)	116.080(6)	87.497(6)	695.83(16)	43
7369m	50.0	49.9	0.1	40/900+20/1000		8.3717(13)	12.9222(11)	7.2011(10)	91.807(11)	116.010(8)	87.476(10)	699.37(22)	46
7326m	55.0	44.9	0.1	40/900+20/1000		8.3949(14)	12.9321(9)	7.2047(10)	91.481(9)	115.973(8)	87.520(8)	702.48(22)	51
8458u	60.0	39.9	0.1	40	1000	8.4195(23)	12.9399(15)	7.2060(21)	91.324(17)	115.934(16)	87.517(12)	705.34(44)	33
7370o	65.0	34.9	0.1	80	900	8.4465(10)	12.9461(9)	7.2085(8)	91.097(9)	115.915(6)	87.568(8)	708.34(17)	50
7370m	70.0	29.9	0.1	80	900	8.4703(8)	12.9492(8)	7.2112(6)	91.000(7)	115.915(5)	87.575(5)	710.78(13)	44
7370u	75.0	24.9	0.1	80	900	8.4910(9)	12.9513(9)	7.2106(6)	90.886(7)	115.926(5)	87.628(7)	712.52(14)	54
7304o	80.0	19.9	0.1	60	900	8.5139(7)	12.9571(8)	7.2149(7)	90.799(7)	115.919(5)	87.637(6)	715.24(13)	60
7377o	85.0	14.9	0.1	72	800	8.5335(8)	12.9600(9)	7.2157(5)	90.768(6)	115.912(5)	87.603(6)	717.15(13)	56
7380o	90.0	9.9	0.1	72	800	8.5540(8)	12.9582(6)	7.2180(6)	90.694(6)	115.920(5)	87.649(5)	718.97(13)	53
7380m	95.0	4.9	0.1	72	800	8.5735(6)	12.9589(6)	7.2187(5)	90.664(5)	115.944(4)	87.652(5)	720.57(11)	54
7377m	99.8	0.1	0.1	(2)**	72/800	8.5903(10)	12.9616(10)	7.2200(8)	90.631(9)	115.960(7)	87.688(8)	722.18(19)	55
7169m	99.9	0.0	0.1	(2)**		8.5907(8)	12.9634(7)	7.2215(6)	90.609(8)	115.946(5)	87.698(7)	722.56(13)	58
7363m	99.9	0.0	0.1	(2)**		8.5915(6)	12.9624(5)	7.2220(5)	90.627(5)	115.946(4)	87.677(4)	722.60(10)	57
8360m	99.9	0.0	0.1	(2)**		8.5925(7)	12.9645(7)	7.2221(6)	90.607(6)	115.955(4)	87.692(6)	722.77(13)	69
7155m	99.9	0.0	0.1	(2)**		8.5917(7)	12.9612(8)	7.2211(5)	90.623(6)	115.945(4)	87.683(5)	722.48(12)	62

* Standard errors are given in parentheses and refer to the last decimal place(s).
** The number in parentheses refers to Tables 2 and 3.

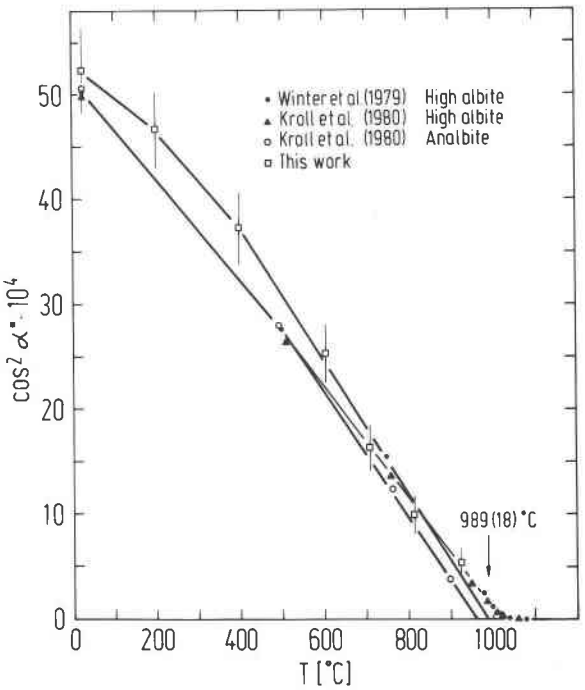

Fig. 1. Variation of $\cos^2\alpha^*$ with temperature for various analbite and high albite samples. Typically the slope of a high albite curve is more gentle than of an analbite curve, because the approach of α^* to 90° is hindered in high albite due to triclinic topochemistry. From the appearance of the curve of heated Cazadero albite it is assumed that monoclinic topochemistry has been achieved. The functions $(\cos^2\alpha^* + \cos^2\gamma) = A$ and $(\cos^2\alpha + \cos^2\gamma^*) = B$ both vary linearly when plotted versus temperature. The cosine terms in each of them are proportional to those off-diagonal elements in the thermal or compositional strain tensor which vanish at the triclinic to monoclinic displacive transformation (Kroll, 1984). Both A and B are related to the square of the order parameter Q for the displacive transformation (Salje et al., 1985). Whether A or B is chosen to represent Q^2, is a matter of convenience. The form of the function—A or B—simply results from the choice of the relative orientation of the crystal axes system to the cartesian system used to express the strain tensor components in terms of lattice parameters. Because $\cos\alpha^*$ is linearly related to $\cos\gamma$ as is $\cos\alpha$ to $\cos\gamma^*$, it suffices to plot either $\cos^2\alpha^*$ or $\cos^2\alpha$ versus temperature.

the Na- and K-end members (200 mg) were then weighed at intervals of 5 mol%, thoroughly mixed in an agate mortar, pressed to tablets (at 1 kbar) and homogenized at 800–1000°C for 40 to 80 hours. Lattice parameters were determined from Guinier–Jagodzinski photographs ($CuK\alpha_1$ radiation) using standard procedures (e.g., Kroll et al., 1980); see Table 4.

In preliminary experiments we had determined the temperature range in which homogenization would proceed, but Al,Si disordering would not. When the lattice parameters of the heated and unheated end members are compared in Table 4 it is seen that they are indeed statistically identical.

Analbite–high sanidine series

A topochemically monoclinic alkali feldspar series in which the Al,Si distribution does not change with composition is best prepared from only one end member which is ion-exchanged to yield the other end member. We did not use sanidine as starting material because Na-exchange typically produces poor powder patterns, whereas K-exchange results in sharp patterns.

We started with Cazadero albite which was converted into analbite by dry heating of crushed fragments (1–5 mm in size) in a sealed platinum tube at 1090°C for 110 days. A single crystal was then X-rayed on the precession camera and the α^* angle followed with temperature. To effectively linearize the variation of α^* we plotted $\cos^2\alpha^*$ vs. T (Thompson et al., 1974; Kroll, 1984), see Figure 1. The straight line drawn through the data points for $T \geq 400$°C intersects the abscissa ($\alpha^* = 90°$) at 989 ± 18°C. For comparison the data points of another analbite and two high albites are also plotted. The analbite and one of the high albites were hydrothermally crystallized from glasses at 1000 and 950°C, respectively (Kroll et al., 1980), whereas the second high albite was prepared by dry heating of Tiburon low albite (Winter et al., 1979). The data points of the two high albites virtually follow the same line, which has a more gentle slope than has the analbite line. This is typical for high albite compared to analbite and results from the fact that the approach to monoclinic geometry is hindered by the topochemically triclinic Al,Si distribution (see Kroll et al., 1980, p. 1200). Thus, the behavior of our heated Cazadero albite in Figure 1 is consistent with, though not proof of the assumption that this Na-feldspar is in fact topochemically monoclinic.

It may be noted that long term annealing at temperatures well above the temperature of the diffusive transformation does not necessarily mean that monoclinic topochemistry has been achieved. Even if the K-exchange product of such a Na-feldspar yields a sharp monoclinic powder pattern, the Al,Si distribution of the original Na-feldspar still may have been topochemically triclinic. We found that after K-exchange two high albites which were hydrothermally synthesized at 950 and 900°C resulted in monoclinic powder patterns, whereas a sample prepared at 850°C yielded a triclinic pattern.

After it had become probable from Figure 1 that our heated Cazadero albite was indeed analbite, it was K-exchanged, analyzed by AAS (Table 3), and a solid solution series was prepared analogous to the LA–LM series. Lattice parameters and homogenization conditions are listed in Table 5.

It is seen from Table 5 that the cell volume of the K-exchanged analbite is significantly larger before than after heating at 1000°C for 2 days, which is surprising. Probably the K-exchange was not quite complete, but due to its small amount the non-exchanged analbite did not show up in the powder pattern, and thus the lattice parameters represent the fully exchanged product. During heating, however, mixing occurred and consequently the cell volume dropped to the value that represents the bulk composition determined by AAS analysis. If a similar effect has occurred in the LA–LM series, it is hidden within the uncertainty of the chemical analysis.

Low ternary feldspar series

Three oligoclase crystals $An_{16.5}$, $An_{21.5}$ and $An_{27.8}$ were K-exchanged, and low ternary feldspar series of constant An-content were prepared using the procedures described above. Details concerning the end members are given in Tables 2 and 3. The lattice parameters and homogenization conditions are listed in Table 6.

High ternary feldspar series

Two oligoclases $An_{16.5}$ and $An_{27.0}$ were converted into the high structural state by dry heating of crushed fragments (1–5 mm in size) in sealed platinum capsules (Tables 2 and 3). Monoclinic

Table 5. Unit cell parameters of analbite–high sanidine solid solutions

Sample No.	Or [mol%]	Ab [mol%]	An [mol%]	Homogenization t[days]	T[°C]	a [Å]	b [Å]	c [Å]	α [°]	β [°]	γ [°]	V [Å^3]	No. lines
7156m	0.3	99.4	0.3	(3)**		8.1560(6)*	12.8713(6)	7.1077(4)	93.483(5)	116.448(4)	90.251(5)	666.41(10)	69
7556m	5.0	94.7	0.3	(3)**2d/1000°C		8.1806(11)	12.8855(18)	7.1137(11)	93.212(13)	116.418(7)	90.246(10)	670.14(20)	42
7556u	10.0	89.7	0.3	2d	1000°C	8.2038(6)	12.9018(6)	7.1213(5)	92.965(5)	116.403(4)	90.203(5)	673.92(10)	52
7560o	14.9	84.8	0.3	2d	1000°C	8.2256(9)	12.9212(9)	7.1288(8)	92.627(9)	116.358(7)	90.193(7)	677.96(17)	44
7560m	19.9	79.8	0.3	2d	1000°C	8.2469(8)	12.9347(9)	7.1342(6)	92.267(9)	116.344(6)	90.152(7)	681.27(14)	42
7560u	24.8	74.9	0.3	2d	1000°C	8.2697(10)	12.9491(9)	7.1433(10)	91.846(9)	116.308(6)	90.138(6)	685.24(20)	40
7565o	29.8	69.9	0.3	2d	1000°C	8.2900(16)	12.9683(16)	7.1500(15)	91.309(13)	116.275(11)	90.087(13)	689.02(33)	28
8458u	39.7	60.0	0.3	3.7d	1000°C	8.3343(10)	12.9893(10)	7.1562(8)	90	116.184(7)	90	695.21(18)	31
7565u	39.7	60.0	0.3	2d	1000°C	8.3327(14)	12.9883(14)	7.1544(11)	90	116.157(9)	90	695.01(24)	23
7575o	44.6	55.1	0.3	2d	1000°C	8.3603(10)	12.9941(12)	7.1596(6)	90	116.134(6)	90	698.27(16)	29
7575m	49.6	50.1	0.3	2d	1000°C	8.3792(10)	12.9992(10)	7.1611(8)	90	116.101(6)	90	700.46(16)	31
7575u	54.5	45.2	0.3	2d	1000°C	8.4061(11)	13.0057(9)	7.1642(6)	90	116.083(6)	90	703.47(14)	39
7776o	59.4	40.3	0.3	2d	1000°C	8.4305(8)	13.0134(8)	7.1659(5)	90	116.057(4)	90	706.26(11)	42
7576m	64.4	35.3	0.3	2d	1000°C	8.4550(7)	13.0172(8)	7.1675(6)	90	116.032(4)	90	708.82(12)	48
7576u	69.3	30.4	0.3	2d	1000°C	8.4748(8)	13.0197(8)	7.1683(7)	90	116.007(6)	90	710.85(14)	50
7583o	74.3	25.4	0.3	2d	1000°C	8.4978(5)	13.0215(6)	7.1697(4)	90	116.008(3)	90	713.02(9)	52
7583m	79.2	20.5	0.3	2d	1000°C	8.5196(7)	13.0236(7)	7.1714(5)	90	116.000(4)	90	715.17(12)	51
7583u	84.2	15.5	0.3	2d	1000°C	8.5395(6)	13.0263(8)	7.1713(5)	90	115.987(4)	90	717.07(10)	47
7589o	89.1	10.6	0.3	2d	1000°C	8.5599(6)	13.0285(7)	7.1750(5)	90	115.994(4)	90	719.22(10)	56
7589m	94.1	5.6	0.3	2d	1000°C	8.5804(6)	13.0313(7)	7.1762(5)	90	116.001(4)	90	721.18(11)	48
7589u	98.8	0.9	0.3	(4)**2d/1000°C		8.5967(7)	13.0314(8)	7.1785(5)	90	116.022(5)	90	722.66(12)	51
7295m	99.7	0	0.3	(4)**		8.6045(10)	13.0306(10)	7.1787(8)	90	116.011(6)	90	723.36(17)	54

* Standard errors are given in parentheses and refer to the last decimal place(s).

** The number in parentheses refers to Tables 2 and 3.

topochemistry cannot be produced in this way because the stability field of monalbite does not extend above An_{15} (Kroll and Baumbauer, 1981). Consequently, triclinic powder patterns resulted after K-exchange. The degree of Al,Si disorder achieved compares to that of plagioclases synthesized by dry crystallization of glasses close to the solidus. The structure of high $An_{27,0}$ has been refined by Kroll (1978).

Solid solution series were prepared from the end members analogous to the LA–LM series. The temperatures at which the mechanical mixtures were homogenized had to be carefully chosen to avoid changing the degree of disorder: When (Na,Ca)-high albites are K-exchanged and then heated at elevated temperatures (e.g., 900°C for An_{27}), they become topochemically monoclinic K-sanidines (see Kroll and Baumbauer, 1981).

The lattice parameters and homogenization conditions are listed in Table 7.

Table 6. Unit cell parameters of three ternary feldspar solid solutions of low structural state

Sample No.	Homogenization t[days]	T[°C]	Ab [mol%]	Or [mol%]	An [mol%]	a [Å]	b [Å]	c [Å]	α [°]	β [°]	γ [°]	V [Å^3]	No. lines
84-2519m	(5)**		82.8	0.7	16.5	8.149(1)*	12.819(1)	7.137(1)	94.01(1)	116.48(1)	88.67(1)	665.7(1)	53
84-2447m	2d/1000°C		73.4	10.1	16.5	8.193(2)	12.840(2)	7.146(2)	93.68(1)	116.32(1)	88.60(1)	672.4(5)	39
84-2507m	2d/1000°C		63.3	20.2	16.5	8.235(1)	12.873(1)	7.155(1)	93.28(1)	116.34(1)	88.58(1)	678.6(2)	32
84-2445u	2d/1000°C		53.2	30.3	16.5	8.284(1)	12.904(1)	7.167(1)	92.80(1)	116.29(1)	88.52(1)	686.4(2)	40
84-2445m	2d/1000°C		43.1	40.4	16.5	8.315(1)	12.918(1)	7.172(1)	92.41(1)	116.19(1)	88.49(1)	690.7(2)	44
84-2445o	2d/1000°C		33.0	50.5	16.5	8.355(1)	12.937(1)	7.179(1)	91.97(1)	116.13(1)	88.45(1)	696.2(1)	40
84-2507o	2d/1000°C		22.9	60.6	16.5	8.389(1)	12.950(1)	7.183(1)	91.63(1)	116.10(1)	88.41(1)	700.6(1)	55
84-5883o	6d/750°C+7d/800°C		12.8	70.7	16.5	8.429(1)	12.962(1)	7.187(1)	91.30(1)	115.98(1)	88.38(1)	705.5(1)	63
84-2384m	(6)**		0	83.5	16.5	8.475(1)	12.974(1)	7.192(1)	91.03(1)	115.93(1)	88.38(1)	710.9(1)	67
166-2519u	(7)**		77.3	1.2	21.5	8.160(1)	12.837(1)	7.133(1)	93.87(1)	116.44(1)	88.96(1)	667.4(1)	38
166-2450m	2d/1000°C		68.5	10	21.5	8.191(1)	12.854(1)	7.140(1)	93.60(1)	116.38(1)	88.91(1)	672.0(2)	41
166-2450o	2d/1000°C		58.5	20	21.5	8.233(1)	12.878(1)	7.148(1)	93.25(1)	116.33(1)	88.86(1)	678.2(2)	42
166-2449u	2d/1000°C		48.5	30	21.5	8.274(2)	12.906(2)	7.158(1)	92.77(1)	116.26(1)	88.80(1)	684.7(3)	28
166-2449m	2d/1000°C		38.5	40	21.5	8.317(2)	12.930(1)	7.166(1)	92.29(1)	116.15(1)	88.76(1)	691.3(3)	35
166-5911u	6d/750°C+7d/800°C		28.5	50	21.5	8.360(1)	12.945(1)	7.172(1)	91.87(1)	116.07(1)	88.68(1)	696.8(2)	52
166-6258m	6d/750°C+7d/800°C		18.5	60	21.5	8.393(2)	12.954(2)	7.175(1)	91.52(1)	116.01(1)	88.67(1)	700.8(3)	37
166-5911o	6d/750°C+7d/800°C		8.5	70	21.5	8.425(1)	12.967(1)	7.181(1)	91.29(1)	115.98(1)	88.66(1)	704.9(2)	50
166-2384u	(8)**		0	78.5	21.5	8.460(1)	12.982(1)	7.185(1)	91.10(1)	115.93(1)	88.63(1)	709.5(2)	51
31-2519o	(9)**		69.9	2.3	27.8	8.158(1)	12.844(1)	7.121(1)	93.75(1)	116.39(1)	89.37(1)	666.8(1)	46
31-2443o	2d/1000°C		62.2	10	27.8	8.192(2)	12.867(1)	7.131(1)	93.49(1)	116.32(1)	89.33(1)	672.4(2)	30
31-6206m	10d/850°C		52.2	20	27.8	8.226(1)	12.888(1)	7.135(1)	93.18(1)	116.28(1)	89.28(1)	677.4(2)	41
31-2442m	2d/1000°C		42.2	30	27.8	8.276(2)	12.917(1)	7.148(1)	92.71(1)	116.21(1)	89.22(1)	684.8(3)	27
31-2442o	2d/1000°C		32.2	40	27.8	8.317(1)	12.938(1)	7.156(1)	92.28(1)	116.16(1)	89.20(1)	690.5(3)	35
31-2441u	2d/1000°C		22.2	50	27.8	8.357(1)	12.957(1)	7.160(1)	91.90(1)	116.12(1)	89.17(1)	695.8(2)	25
31-5926m	6d/750°C+7d/800°C		12.2	60	27.8	8.380(1)	12.965(1)	7.163(1)	91.69(1)	116.00(1)	89.10(1)	699.2(2)	61
31-2423o	(10)**		0	72.2	27.8	8.424(1)	12.983(1)	7.170(1)	91.37(1)	115.95(1)	89.06(1)	704.9(1)	50

* Standard errors are given in parentheses and refer to the last decimal place.

** The number in parentheses refers to Tables 2 and 3.

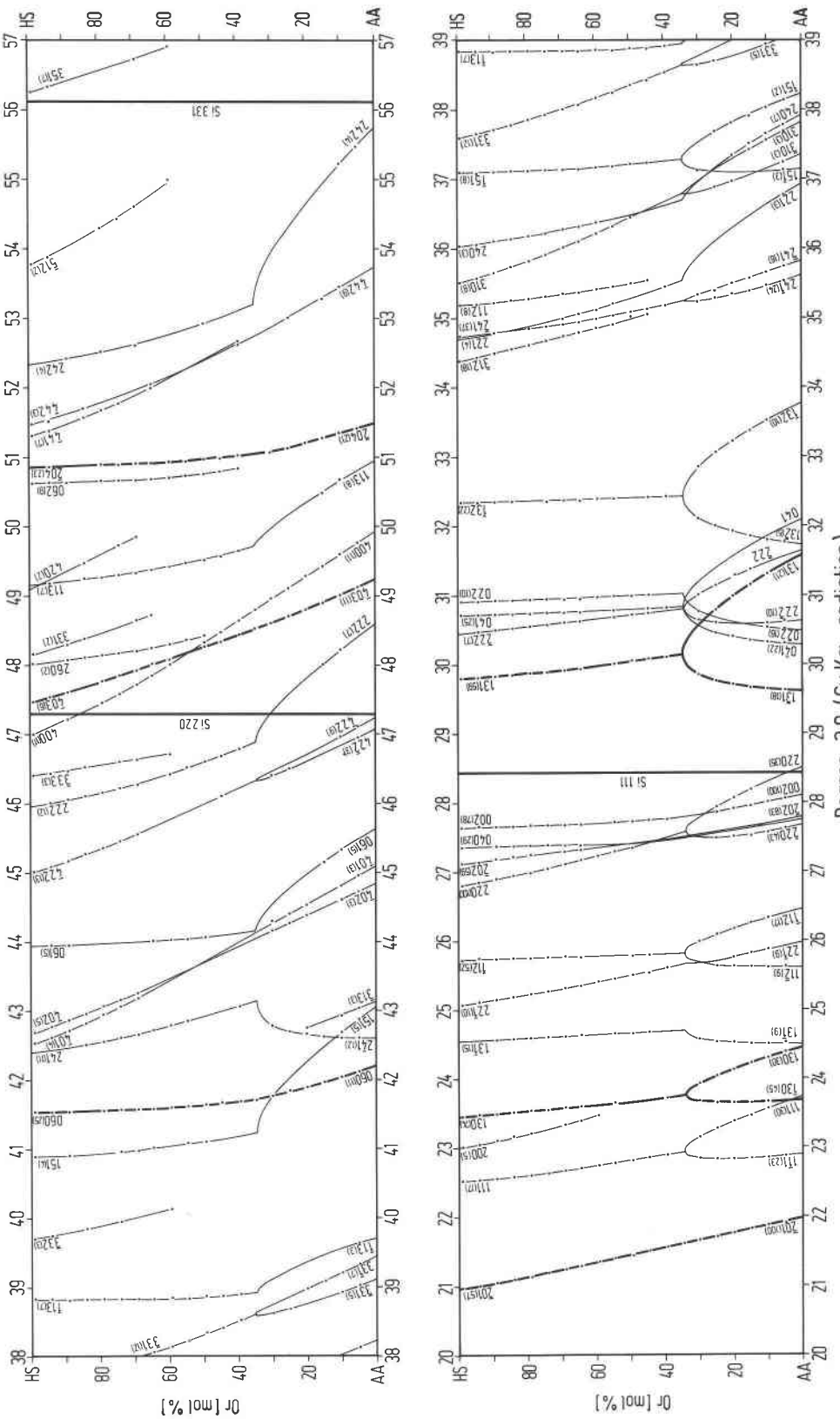

Fig. 2. Indexing chart for the analbite (AA)–high sanidine (HS) series. For practical purposes, only those lines are plotted that have actually been used for lattice parameter refinement (indicated by dots). Numbers following Miller indices are relative intensities, based on a scale of 100 (Borg and Smith, 1969). Diagnostically important lines and lines for the Si internal standard are drawn heavily.

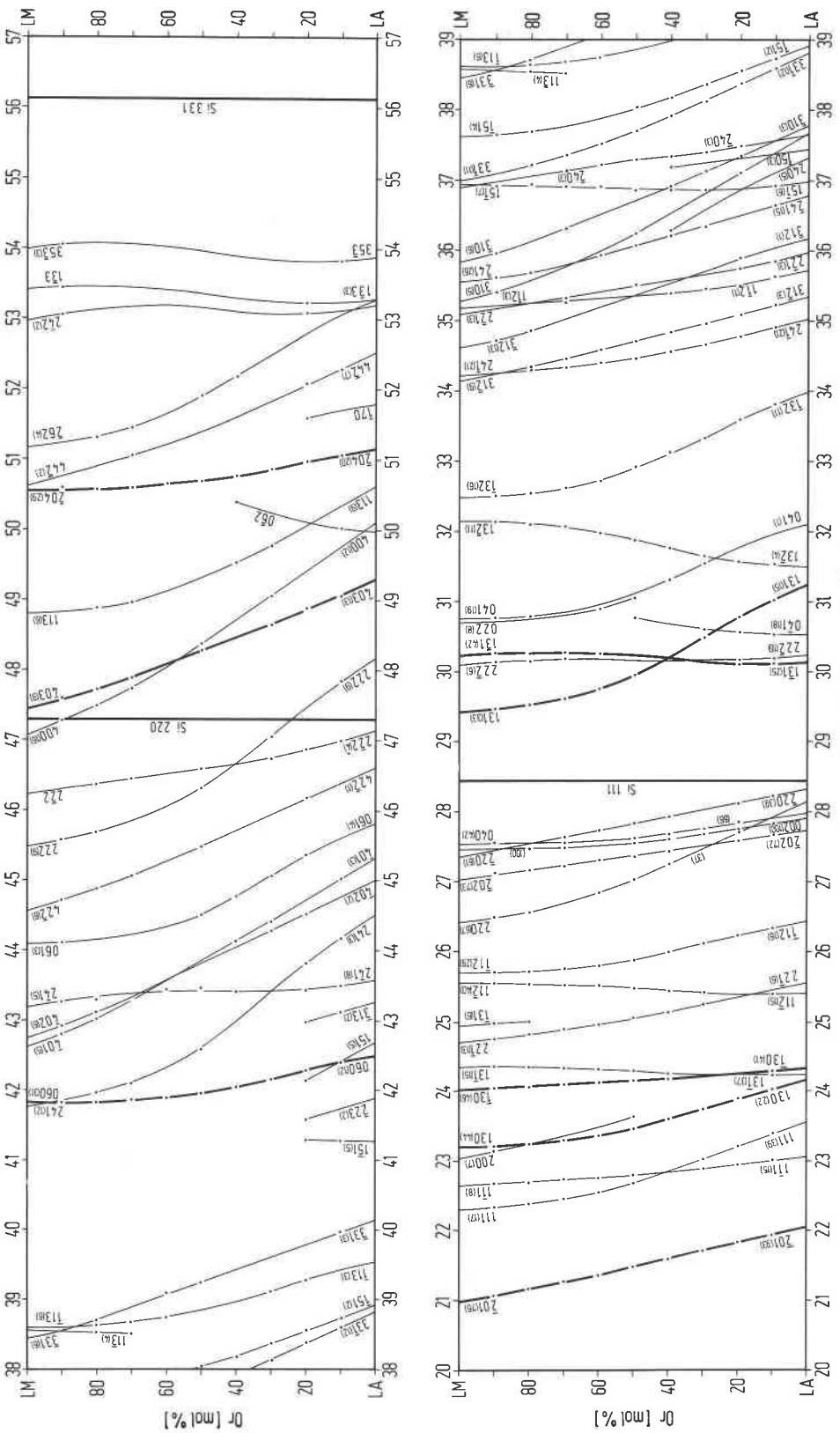

Fig. 3. Indexing chart for the low albite (LA)–low microcline (LM) series. See Fig. 2 for explanation.

Table 7. Unit cell parameters of two ternary feldspar solid solutions of high structural state

Sample No.	Homogenization t[days] T[°C]	Ab [mol%]	Or [mol%]	An [mol%]	a [Å]	b [Å]	c [Å]	α [°]	β [°]	γ [°]	V [Å³]	No. lines
Vis-4973m	(11)**	79	4.5	16.5	8.170(1)*	12.879(1)	7.114(1)	93.33(1)	116.34(1)	90.25(1)	669.3(1)	47
Vis-5425o	(11)** 18d/850°C	79	4.5	16.5	8.171(1)	12.882(1)	7.112(1)	93.30(1)	116.35(1)	90.26(1)	669.4(1)	84
Vis-5425m	18d/850°C	73.5	10	16.5	8.192(1)	12.893(1)	7.118(1)	93.12(1)	116.33(1)	90.23(1)	672.5(1)	62
Vis-5425u	18d/850°C	63.5	20	16.5	8.232(1)	12.923(1)	7.129(1)	92.62(1)	116.29(1)	90.19(1)	679.0(1)	58
Vis-5434o	18d/850°C	53.5	30	16.5	8.277(3)	12.949(1)	7.139(1)	91.97(1)	116.21(1)	90.11(1)	686.0(4)	33
Vis-5602o	18d/750°C+24d/800°C	43.5	40	16.5	8.311(1)	12.977(1)	7.148(1)	91.11(1)	116.15(1)	90.05(1)	691.9(2)	31
Vis-5602m	18d/750°C+24d/800°C	33.5	50	16.5	8.355(2)	12.991(1)	7.156(1)	90.30(1)	116.09(1)	89.96(1)	697.6(3)	33
Vis-5602u	18d/750°C+24d/800°C	23.5	60	16.5	8.389(3)	13.002(1)	7.159(1)	90.19(1)	116.09(1)	89.95(2)	701.3(4)	25
Vis-5438m	18d/750°C	13.5	70	16.5	8.442(2)	13.014(1)	7.163(1)	90.15(1)	116.00(1)	89.92(1)	707.3(3)	30
Vis-5438u	18d/750°C	3.5	80	16.5	8.480(1)	13.023(1)	7.167(1)	90.09(1)	115.95(1)	89.95(1)	711.7(2)	37
Vis-5446m	(12)** 18d/750°C	0	83.5	16.5	8.492(1)	13.025(1)	7.170(1)	90.12(1)	115.93(1)	89.94(1)	713.2(3)	25
Vis 5049m	(12)**	0	83.5	16.5	8.496(1)	13.023(1)	7.167(1)	90.11(1)	115.92(1)	89.92(1)	713.2(1)	37
31h-557m	(13)**	67.5	5.5	27	8.177(1)	12.881(1)	7.111(1)	93.31(1)	116.28(1)	90.26(1)	670.1(1)	69
31h-561m	(13)**	67.5	5.5	27	8.177(1)	12.881(1)	7.111(1)	93.31(1)	116.28(1)	90.26(1)	670.1(1)	65
31h-4612o	(13)** 18d/850°C	67.5	5.5	27	8.172(1)	12.878(1)	7.110(1)	93.33(1)	116.28(1)	90.26(1)	669.3(1)	48
31h-4612m	18d/850°C	60.1	12.9	27	8.199(1)	12.896(1)	7.117(1)	93.09(1)	116.25(1)	90.22(1)	673.5(1)	76
31h-4612u	18d/850°C	50.4	22.6	27	8.239(1)	12.920(1)	7.126(1)	92.67(1)	116.24(1)	90.18(1)	679.4(2)	48
31h-4615o	18d/850°C	40.7	32.3	27	8.277(1)	12.947(1)	7.137(1)	92.08(1)	116.13(1)	90.12(1)	686.1(2)	48
31h-4615m	18d/800°C	31.1	41.9	27	8.318(1)	12.975(2)	7.144(1)	91.46(1)	116.11(1)	90.06(1)	692.1(2)	37
31h-4615u	18d/750°C	21.4	51.6	27	8.361(2)	12.993(2)	7.151(1)	90.69(1)	116.00(1)	89.96(2)	698.1(3)	29
31h-4618o	18d/750°C	11.8	61.2	27	8.399(2)	13.000(1)	7.154(1)	90.45(1)	115.80(1)	89.93(1)	703.3(4)	34
31h-4618m	(14)** 18d/750°C	0	73	27	8.436(1)	13.012(1)	7.162(1)	90.24(1)	115.93(1)	89.89(1)	707.1(2)	42
31h-4476m	(14)**	0	73	27	8.434(1)	13.009(1)	7.159(1)	90.31(1)	115.92(1)	89.88(1)	706.5(2)	46

* Standard errors are given in parentheses and refer to the last decimal place.

** The number in parentheses refers to Tables 2 and 3.

Results

Indexing charts

As an aid in indexing we prepared two charts for the AA–HS and LA–LM series which give the variation with composition of line positions in the powder pattern (Fig. 2, 3). Only those lines were selected on which we have based the refinement of lattice parameters. This choice should help to avoid misindexing by confusion with lines which are usually too weak to be observed or suffer from overlap. The two charts add to those compiled by Ribbe (1983).

Table 8. Al,Si distribution in the alkali and ternary feldspar solid solutions

No.	Series	t_1o	t_1m	t_2o	t_2m
(1)	LA - LM series	1.00	0.00	0.00	0.00
(2)	AA - HS series	0.28	0.28	0.22	0.22
		t_1o	$<t_1m>$*		
(3)	$Ab_x An_{16.5} Or_{100-x}$ (low)	0.820	0.115		
(4)	-- $An_{21.5}$ -- (low)	0.765	0.150		
(5)	-- $An_{27.8}$ -- (low)	0.675	0.200		
(6)	-- $An_{16.5}$ -- (high)	0.350	0.270		
(7)	-- $An_{27.0}$ -- (high)	0.395	0.290		

(1) t-values derived from structure refinements (Cazadero-LA: Wenk and Kroll (1984), Prilep-LM: Strob (1983))
(2) see discussion by Kroll and Ribbe (1983, p.71,74)
(3)-(7) t-values derived from lattice parameters (Kroll, 1983, Table 1, eq. (iii), p.112)
* $<t_1m> = (t_1m + t_1o + t_2o)/3$

Lattice parameters and Al,Si distribution

Due to the methods of synthesis, the Al,Si distribution in each of the seven solid solution series remains constant. This has been determined by structure refinement or from lattice parameters by applying the equations given by Kroll and Ribbe (1983) and Kroll (1983). These equations apply to alkali feldspars, plagioclases and ternary feldspars. The results are listed in Table 8.

Instead of refining the whole set of lattice parameters to determine the Al,Si distribution, it is also possible to use just two or three lines of the powder pattern. To characterize the "triclinicity" of microclines Goldsmith and Laves (1954) and MacKenzie (1954) suggested the use of 131–1$\bar{3}$1 and 130–1$\bar{3}$0 line splittings, respectively. Wright (1968) proposed the "three-peak-method" for the alkali feldspars, which is analogous to the b^*, c^* plot of Smith (1974, p. 258). Based on the data presented in this paper, Kroll and Ribbe (in prep.) give improved and modified diagrams and equations related to these simple determinative methods.

The unit cell parameters of the two alkali feldspar series are plotted in Figure 4. Their variation with composition and structural state is discussed by Kroll and Ribbe (1983), also see Kroll et al. (1980), Kroll (1984), and citations therein. We will only briefly compare the variation of the α and γ angles in the various series.

In topochemically triclinic alkali feldspars, α and γ deviate from 90° for two reasons: (a) the double crankshafts are twisted (displacive effect), (b) the Al,Si distribution is unbalanced with respect to the T_10, T_1m and T_20, T_2m sites. When such a structure is rapidly heated or Na is replaced by K, only the displacive part of the "triclinicity"

Table 9. Polynomials to calculate from cell volume V or line positions $2\theta(\bar{2}01)$ and $2\theta(400)$ mole fraction Or: $n_{Or} = A + BX + CX^2 + DX^3$

A	B	C	D	X (1)	r^2 (2)	s.e.e. (3)	End member composition
AA - HS series							
-535.189	2.37332	$-3.52656\cdot10^{-3}$	$1.75615\cdot10^{-6}$	V	0.9999	0.003	$Or_0 - Or_{100}$
956.454	$-1.29628\cdot10^{2}$	5.89731	$-9.00579\cdot10^{-2}$	$2\theta(\bar{2}01)$	0.9997	0.005	
1331.715	$-8.08172\cdot10^{1}$	1.64116	$-1.11502\cdot10^{-2}$	$2\theta(400)$	0.9998	0.005	
LA - LM series							
-1209.141	5.28104	$-7.70522\cdot10^{-3}$	$3.75650\cdot10^{-6}$	V	0.9999	0.004	$Or_0 - Or_{100}$
2835.280	$-3.91584\cdot10^{2}$	$1.80689\cdot10^{1}$	$-2.78524\cdot10^{-1}$	$2\theta(\bar{2}01)$	0.9999	0.004	
1973.637	$-1.19995\cdot10^{2}$	2.43771	$-1.65450\cdot10^{-2}$	$2\theta(400)$	0.9999	0.004	
Intermediate series (4)							
-872.330	3.82791	$-5.61695\cdot10^{-3}$	$2.75683\cdot10^{-6}$	V			$Or_0 - Or_{100}$
1893.263	$-2.60243\cdot10^{2}$	$1.19662\cdot10^{1}$	$-1.84028\cdot10^{-1}$	$2\theta(\bar{2}01)$			
1652.359	$-1.00387\cdot10^{2}$	2.03905	$-1.38450\cdot10^{-2}$	$2\theta(400)$			
High ternary feldspar series							
-290.385	1.29420	$-1.94416\cdot10^{-3}$	$9.84369\cdot10^{-7}$	V	0.9994	0.008	$Ab_{83.5}An_{16.5} - Or_{83.5}An_{16.5}$
-3663.318	$1.60097\cdot10^{1}$	$-2.33406\cdot10^{-2}$	$1.13527\cdot10^{-5}$	V	0.9989	0.009	$Ab_{73.0}An_{27.0} - Or_{73.0}An_{27.0}$
Low ternary feldspar series							
-84.613	$4.26086\cdot10^{-1}$	$-7.26319\cdot10^{-4}$	$4.16429\cdot10^{-7}$	V	0.9992	0.008	$Ab_{83.5}An_{16.5} - Or_{83.5}An_{16.5}$
-1192.436	5.23476	$-7.68191\cdot10^{-3}$	$3.76914\cdot10^{-6}$	V	0.9986	0.010	$Ab_{78.5}An_{21.5} - Or_{78.5}An_{21.5}$
-1329.274	5.88082	$-8.69398\cdot10^{-3}$	$4.29549\cdot10^{-6}$	V	0.9984	0.010	$Ab_{72.2}An_{27.8} - Or_{72.2}An_{27.8}$

(1) V is measured in $Å^3$, 2θ-values refer to $CuK\alpha_1$-radiation (λ = 1.540598 Å), (2) r^2 = coefficient of determination, (3) s.e.e. = standard error of estimate, (4) polynomials calculated for curves that lie halfway between the limiting analbite (AA) - high sanidine (HS) and low albite (LA) - low microcline (LM) curves.

the structural state is known and the proper determinative curve can be chosen.

The influence of An-content on estimating n_{Or} from volume is shown in Figure 8. Only the high and the low $An_{16.5}$ ternary series are compared to the alkali feldspars, because other ternary series almost coincide with these two. A decrease in volume with increasing An-content in disordered alkali feldspars is observed, especially for Or-rich compositions, and thus should be considered, if possible. An-content can be determined from a powder pattern using Viswanathan's (1971, 1972) ion-exchange technique. (See Kroll, 1983, Fig. 5, for a compilation of the determinative diagrams of Viswanathan, 1971 and Johannes, 1979.) Polynomials to estimate n_{Or} from V in the ternary series are given in Table 9.

Margules volume parameters

Margules parameters are widely used to describe the deviation from ideal behavior in solid solutions. The Margules volume parameters were defined by Thompson (1967, p. 352) as

$$W_{V(Ab)} = \bar{V}^*_{Ab} - \bar{V}_{Ab} \quad (1)$$

and

$$W_{V(Or)} = \bar{V}^*_{Or} - \bar{V}_{Or}, \quad (2)$$

where $\bar{V}^*_{Ab}$ ($\bar{V}^*_{Or}$) is the partial molar volume of Ab (Or) at infinite dilution in Or (Ab), and $\bar{V}_{Ab}$ ($\bar{V}_{Or}$) is the molar volume of pure Ab (Or). $\bar{V}^*_{Ab}$ and $\bar{V}^*_{Or}$ can be calculated from the equations

$$\bar{V}^*_{Ab} = \bar{V}_{Or} + \left(\frac{\partial \bar{V}}{\partial n_{Ab}}\right)_{n_{Ab}=0} \quad (3)$$

and

$$\bar{V}^*_{Or} = \bar{V}_{Ab} + \left(\frac{\partial \bar{V}}{\partial n_{Or}}\right)_{n_{Or}=0}, \quad (4)$$

see Waldbaum and Thompson (1968, equation 6). The Margules parameters can thus be found via equations (1)–(4) from a least-squares fit of a polynomial of $\bar{V}$ in n_{Or}:

$$\bar{V} = A + Bn_{Or} + Cn^2_{Or} + Dn^3_{Or} + \ldots . \quad (5)$$

If $\bar{V}$ can be expressed as a second or third order polynomial, it is convenient to formulate $\bar{V}$ in terms of $W_{V(Ab)}$ and $W_{V(Or)}$ in order to directly get the Margules parameters and their standard errors (Waldbaum and Thompson, 1968, equation 10):

$$\bar{V} = \bar{V}_{Ab}n_{Ab} + \bar{V}_{Or}n_{Or} + W_{V(Or)}n^2_{Ab}n_{Or} + W_{V(Ab)}n_{Ab}n^2_{Or}. \quad (6)$$

Applying equation (6), Hovis (1977) and Hovis and Peck-

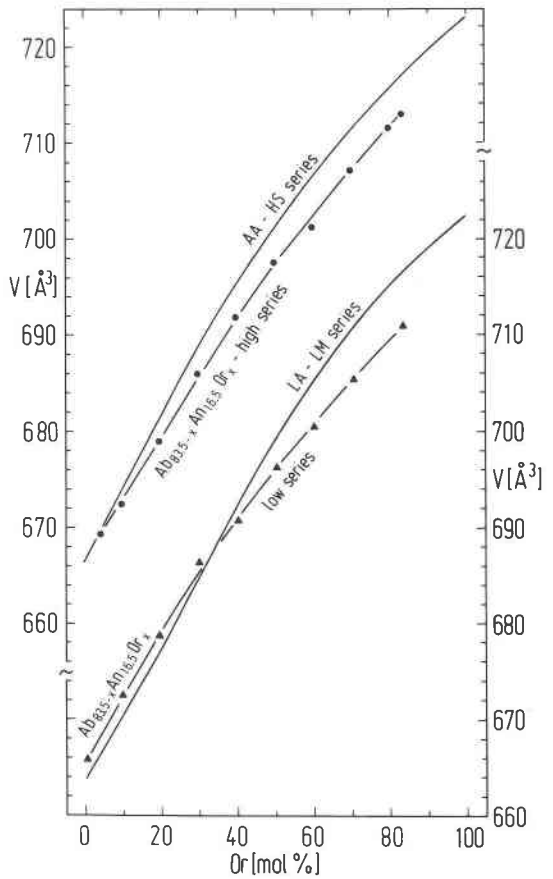

Fig. 8. Comparison of the volume curves of disordered and ordered alkali and ternary feldspar series demonstrating the influence of An-content on volume.

ins (1978) concluded that no more than a symmetric fit with $W_{V(Ab)} = W_{V(Or)}$ is justified in both the AA–HS and LA–LM series. Based on the precision and density of the new data we can modify this conclusion.

The AA–HS series is a non-isostructural series consisting of two populations, the triclinic K-analbites and the monoclinic Na-sanidines. It has, however, for the most part been treated as a single series because of insufficient data. We will subdivide the series into two portions, Or_0–$Or_{29.8}$ and $Or_{39.7}$–Or_{100}, and fit them separately using equation (5). In deciding what degree of polynomial should be chosen we applied the F-value criterion: the F statistic had a maximum for the chosen polynomial and dropped when the degree was further increased.

The Na-sanidine data in Figure 4 are adequately described by a parabola, whereas the K-analbite data follow a straight line (see Table 10 for polynomial coefficients). A straight line, however, would imply ideal volume behavior; and furthermore, extrapolation to Or_{100} would yield a volume for hypothetical triclinic sanidine far greater than the true value for sanidine. Both consequences appear to be improbable. However, a parabolic fit is not justified statistically: not only did the F-value drop, but also the Student-|t|-value of the coefficient of the quadratic term became smaller than 1.

On the other hand, extrapolation of the K-sanidine parabola, which comprises two-thirds of the total data, results in a reasonable volume for hypothetical room-temperature monalbite: $\bar{V} = 2.4047$ cal/bar or $V = 668.25$ Å^3 compared with $\bar{V} = 2.3976$ cal/bar or $V = 666.28$ Å^3 for analbite. Thus, reduction in symmetry at room temperature would decrease the cell volume by about 2 Å^3.

In a strict sense, each of the two subseries requires its own Margules parameters. For the K-analbite series W_V would equal zero because of the straight line fitting, whereas for the Na-sanidine series we calculate from polynomial (4) in Table 10 W_V (RT − monalbite) = W_V (high sanidine) = 0.077(7) cal/bar. However, the accuracy of these Margules parameters is considered low because of the uncertainty inherent in the extrapolation, especially for the K-analbite series. We therefore approximate the molar volumes of the hypothetical end members, namely triclinic sanidine and room-temperature monalbite, by the actual molar volumes of high sanidine and analbite. This implies approximation of the AA–HS series as an isostructural series. Using equations (1) to (4), we find from the polynomials in Table 10

$$W_{V(AA)} = A_4 + B_4 - A_3 = 0.084(4) \text{ cal/bar}; \quad (7)$$

Table 10. Polynomials relating molar volume V [cal/bar] to mole fraction Or or Ab: $\bar{V} = A + BX + CX^2 + DX^3$

		A	B	C	D	X	$r^{2(1)}$	s.e.e.$^{(2)}$
	LA - LM series							
(1)	Or_0 - Or_{35}	2.3882(7)$^{(3)}$	0.2263(88)	0.0875(232)	-	n_{Or}	0.9990	0.0011
(2)	Or_{35} - Or_{100}	2.5997(4)	-0.1181(59)	-0.0566(227)	-0.0785(230)	n_{Ab}	0.9998	0.0007
	AA - HS series							
(3)	Or_0 - $Or_{29.8}$	2.3976(4)	0.2748(24)	-	-	n_{Or}	0.9996	0.0006
(4)	$Or_{39.7}$ - Or_{100}	2.6024(5)	-0.1208(41)	-0.0769(65)	-	n_{Ab}	0.9995	0.0009

(1) r^2 = coefficient of determination, (2) s.e.e. = standard error of estimate,
(3) errors are given in parentheses and refer to the last decimal places.
To convert molar volume $\bar{V}$[cal/bar] to cell volume V[Å^3] divide $\bar{V}$ by 0.0035985.

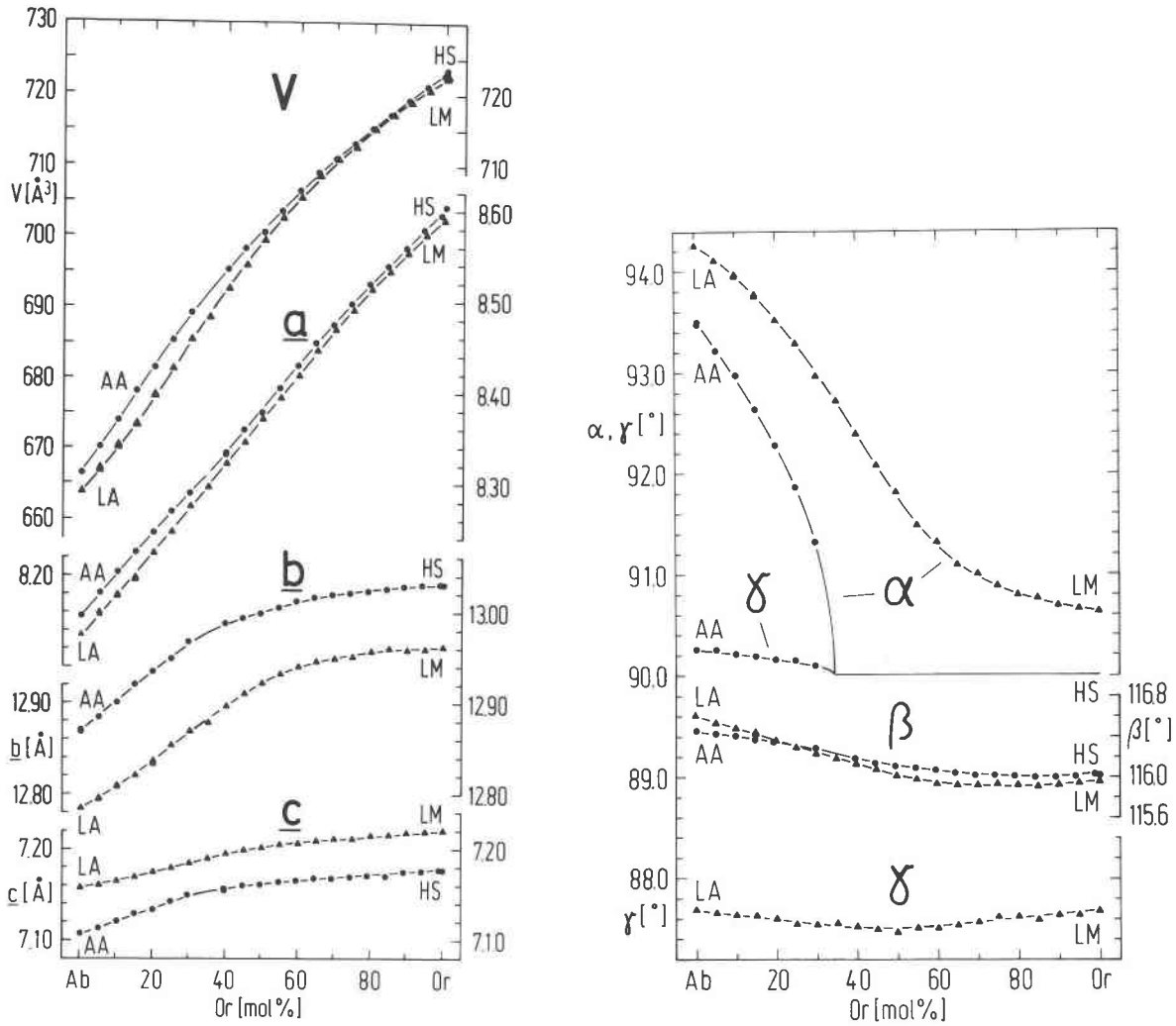

Fig. 4. Unit cell parameters of the analbite (AA)–high sanidine (HS) and low albite (LA)–low microcline (LM) series.

decreases, but the remaining diffusive portion prevents α and γ from reaching 90°. This is true for the two ternary high series, in which α and γ only approach 90°, but do not reach it, in contrast to the topochemically monoclinic AA–HS series (Figs. 4 and 5).

The α and γ angles deviate from 90° to a larger extent in the An_{27} high series than they do in the $An_{16.5}$ series: γ reflects the greater unbalance of the Al-content on the $T_1$0 and T_1m sites of An_{27}, whereas α shows the influence of the larger Ca-content, by which the displacive effect becomes larger.

The displacive effect taken alone increases both α and γ to values greater than 90°, whereas Al,Si ordering increases α, but decreases γ. Therefore, both angles become smaller—regardless of structural state—when upon heating or substitution the displacive influences are reduced. This is also seen in the low ternary series (Fig. 5), where γ deviates more from 90° with increasing K-content. When the displacive influence on γ is finally removed at a sufficiently large K-content, γ will increase towards 90° with a further increase in K-content. This point is not reached in the ternary series but occurs in the LA–LM series at $\sim Or_{40}$.

Displacive transformation

The Or-content at which the displacive transformation occurs in the AA–HS series can be found from a plot of $\cos^2\alpha$ versus composition (see caption to Fig. 1). Figure 6 indicates Or_{displ} = 34.4 mol%, which compares well with the results of Hovis (1980), Kroll et al. (1980) and Harlow (1982) on both natural and synthetic topochemically monoclinic series.

Estimation of Or-content

The cell volume (V) of alkali feldspars is a convenient measure of their Or-content (n_{Or}). Orville's (1967) formula is widely used, although it was derived from synthetic K-sanidines only; however, for simplicity its use for all alkali feldspars regardless of structural state was suggested by Stewart and Wright (1974). The LA–LM and AA–HS

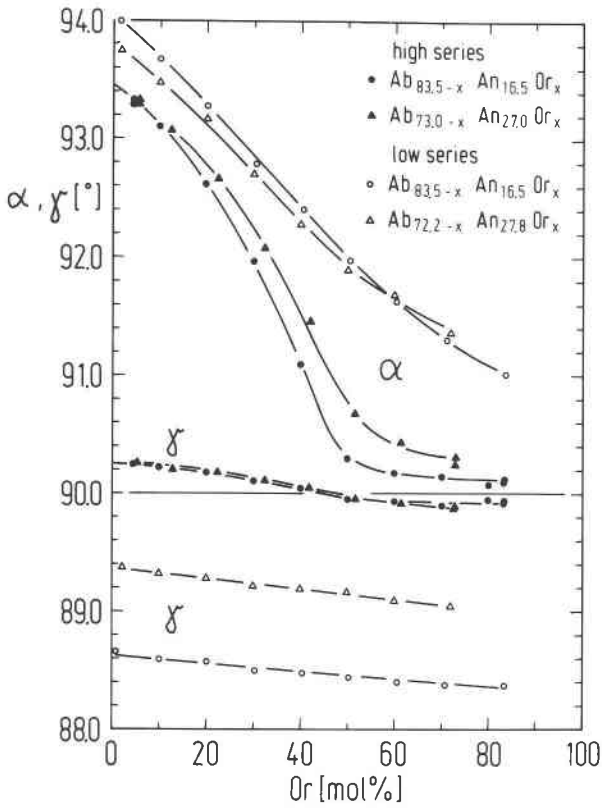

Fig. 5. Variation with composition of the lattice angles α and γ in the high and low ternary feldspar series.

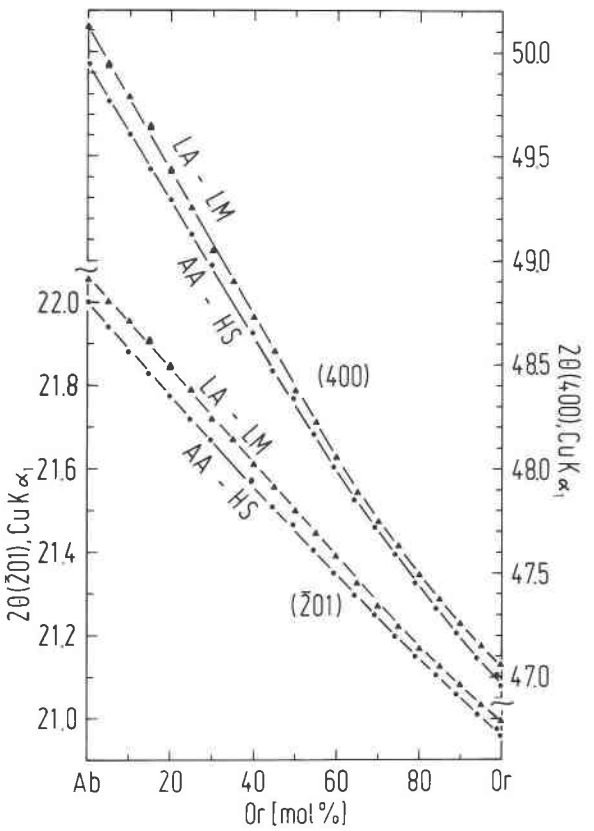

Fig. 7. Line positions of $2\theta(\bar{2}01)$ and $2\theta(400)$, Cu$K\alpha_1$-radiation, versus composition in the analbite (AA)–high sanidine (HS) and low albite (LA)–low microcline (LM) series.

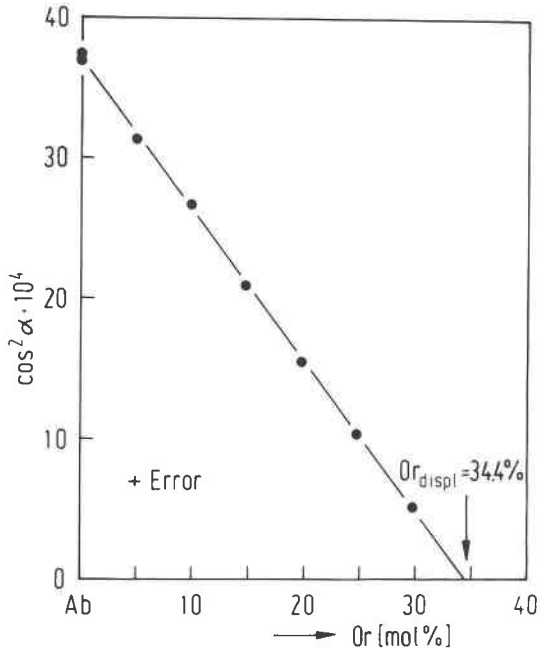

Fig. 6. Variation of $\cos^2\alpha$ in the K-analbite part of the analbite (AA)–high sanidine (HS) series. The displacive transformation occurs at 34.4 mol% Or.

series of this paper provide an improved estimate of Or-content. Volume curves for both series are drawn in Figure 4, and equations were calculated to derive n_{Or} from them. The coefficients are listed in Table 9, to which curves have been added that are midway between the extremes and are useful for intermediate or unknown structural states.

The polynomials in Table 9 are based on a larger body of data than were those given by Kroll and Ribbe (1983, p. 74), and thus the coefficients differ. The resulting values of n_{Or}, however, are virtually the same.

We have calculated the polynomials with mol fraction Or as the dependent variable. It is clearly more meaningful physically to consider $V = f(n_{Or})$ rather than $n_{Or} = f(V)$. However, from a statistical point of view both variables are subject to random error and thus neither of them is preferred to the other. Because we want to find n_{Or} from V, we have used the version with V being the independent variable.

A much simpler though less accurate method to estimate n_{Or} is to use the positions of the $(\bar{2}01)$ or (400) peaks in a powder pattern (Orville, 1967; also see Smith, 1974, p. 280 ff). Figure 7 gives the variation of $2\theta(\bar{2}01)$ and $2\theta(400)$ within both series. The appropriate polynomials are listed in Table 9. An error of 0.01° in $2\theta(\bar{2}01)$ or 0.025° in $2\theta(400)$ produces an error of ~1 mol% Or, provided

Table 11. Margules volume parameters W_V[cal/bar] of the analbite (AA)–high sanidine (HS) and low albite (LA)–low microcline (LM) series calculated from the polynomials listed in Table 10

	$W_{V(Ab)}$		$W_{V(Or)}$	Reference
AA	0.084(4)*	HS	0.070(2)	this work
AA	0.086(4)	HS	0.086(4)	Hovis (1977)
LA	0.093(6)	LM	0.015(9)	this work
LA	0.078(4)	LM	0.078(4)	Hovis & Peckins (1978)

* Errors are given in parentheses and refer to the last decimal place.

$$W_{V(HS)} = A_3 + B_3 - A_4 = 0.070(2) \text{ cal/bar}. \quad (8)$$

When fitting the LA–LM series it was found that a third-order polynomial still resulted in a markedly systematic distribution of residuals. Even a fourth-order polynomial was inadequate because of lack of fit near the end members. It is critical, however, in deriving the Margules parameters to model the slope of the volume curve near the end members as faithfully as possible. We thus divided the LA–LM series into two parts and fitted them separately by second and third order polynomials (Table 10), from which we find

$$W_{V(LA)} = A_2 + B_2 - A_1 = 0.093(6) \text{ cal/bar}; \quad (9)$$
$$W_{V(LM)} = A_1 + B_1 - A_2 = 0.015(9) \text{ cal/bar}. \quad (10)$$

The Margules parameters are compiled in Table 11 and the values given recently by Hovis (1977) and Hovis and Peckins (1978) are added for comparison. It is seen that $W_{V(Ab)}$ and $W_{V(Or)}$ definitely differ from each other in the LA–LM series, and they also differ from those of Hovis and Peckins (1978), which is a consequence of the symmetric fit chosen by them. In the AA–HS series the W_V values are similar to each other and similar to Hovis (1977) symmetric fit. It is thus apparent that the Al,Si distribution does affect the Margules parameters. Increasing order causes $W_{V(Ab)}$ to increase slightly, but $W_{V(Or)}$ is decreased strongly. This finding is discussed in the next section.

The errors in W_V given in Table 11 appear to be larger than would be expected from the smooth volume curves in Figure 4. They have to be attributed to the fact that we have decided to represent the AA–HS and LA–LM series by two polynomials each: the smaller the sample size, the larger are the errors in the coefficients. In addition, the errors in W_V are accumulated due to the error propagation law, applied to equation (7)–(10).

The excess volume can be calculated from the polynomials in Table 10. It is displayed in Figure 9, which graphically shows the slightly asymmetric deviation in the AA–HS series and the marked asymmetric behavior in the LA–LM series. Figure 9 contrasts with similar diagrams published previously, which had to be based on a smaller number of data, but is in agreement with the interpretation of Orville's (1967) data by Newton and Wood (1980, Fig. 3).

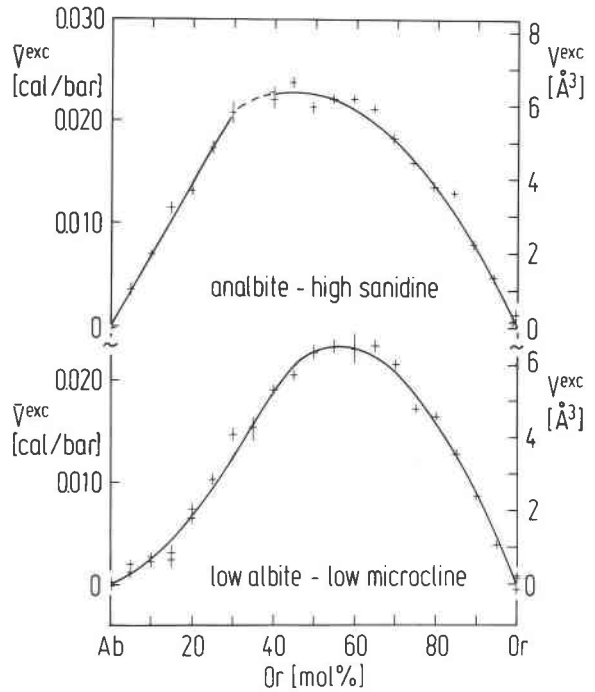

Fig. 9. Excess volume in the analbite (AA)–high sanidine (HS) and low albite (LA)–low microcline (LM) series. Curves are drawn using polynomials given in Table 10. Error bars correspond to one standard deviation.

Volume behavior

The relationship between volume and composition in metal and oxide solid solution series is discussed by v. Steinwehr (1967). He attributes the deviation from ideal (linear) behavior to two factors: (1) geometrical dilatation due to the difference in size of the substituting species, and (2) chemical contraction due to their chemical interactions.

The first factor is trivial and is illustrated by v. Steinwehr (1967) by randomly packing spheres of two different sizes: On the whole the interstices around the spheres are larger than in a packing of equally sized spheres. This effect would also be present in more complicated structures and is therefore responsible for the frequently observed positive excess volumes.

The dilatational effect is counteracted if interactions like ordering or clustering occur within the sphere packing. This second, contractive factor would decrease the positive excess volume, eventually leading to negative values. Newton and Wood (1980) point out that this commonly occurs with silicate solid solutions near their small-volume end member such that a sigmoidal volume-composition curve results. Their interpretation follows the suggestion by Iiyama (1974) who "developed an 'excluded volume' principle, in which an odd-sized trace-element ion deforms the local structure around it . . . and makes it less probable for another trace ion to enter the structure in its immediate neighborhood" (Newton and Wood, 1980, p. 735).

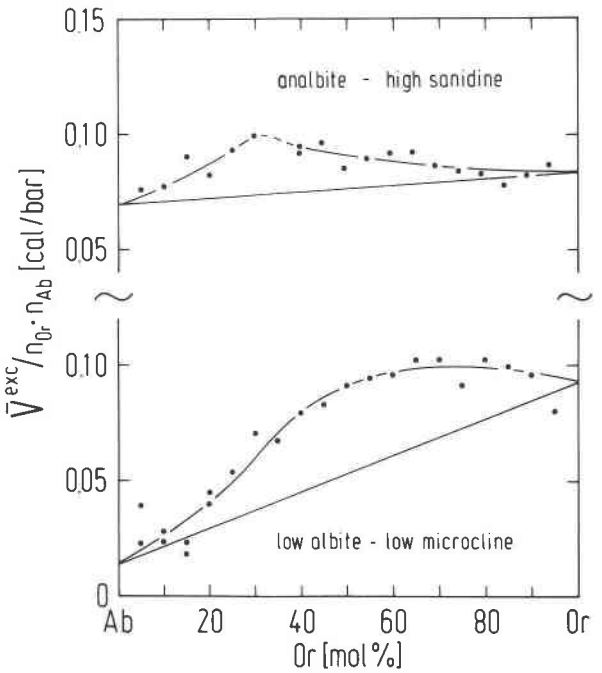

Fig. 10. Variation of normalized excess molar volume $\phi(\bar{V}_{Ab} + \bar{V}_{Or}) = \bar{V}_{exc}/n_{Or}n_{Ab}$ in the analbite (AA)–high sanidine (HS) and low albite (LA)–low microcline (LM) series. Curves are drawn using polynomials in Table 10.

Figure 4 shows that a sigmoidal volume curve does exist in the LA–LM series, which relates to the small excess volumes of Ab-rich compositions in Figure 9. In the AA–HS series the volume curve does not show a sigmoidal shape, whereas Newton and Wood (1980, Fig. 4) found such a shape for Orville's (1967) high albite–high sanidine data. But there the sigmoidal appearance may be caused by the change from monoclinic to triclinic topochemistry near Or_{10}, which does not occur in the AA–HS series (see Fig. 4 of Waldbaum and Thompson, 1968).

v. Steinwehr (1967) suggested the use of composition-dependent normalization of the excess volume as a parameter which is more sensitive to deviations from ideality than is volume and excess volume. Briefly, his reasoning is as follows: In a binary compound A_xB_y ($x + y = 1$), in which A and B are statistically distributed, atomic pairs occur in the ratio

$$n_{AA} : n_{AB} : n_{BB} = x^2 : 2xy : y^2 \qquad (11)$$

A volume element consisting of an average pair of atoms can then be approximated by

$$v_{(AB)} = x^2v_{AA} + 2xyv_{AB} + y^2v_{BB}. \qquad (12)$$

If the A and B atoms are not statistically distributed due to a tendency to ordering or clustering, equation (12) is modified to become

$$v_{(AB)} = (x^2 - \delta)v_{AA} + 2(xy + \delta)v_{AB} + (y^2 - \delta)v_{BB}. \qquad (13)$$

The deviation from ideality, i.e., $v_{AB} \neq (v_{AA} + v_{BB})/2$, is accounted for by a factor ψ such that

$$v_{AB} = (1 + \psi)(v_{AA} + v_{BB})/2. \qquad (14)$$

Inserting equation (14) into (13) and considering that $x^2 = x - xy$ and $y^2 = y - xy$ we have

$$v_{(AB)} = xv_{AA} + yv_{BB} + (xy + \delta)\psi(v_{AA} + v_{BB}). \qquad (15)$$

Since the value of δ is unknown $(xy + \delta)\psi$ is substituted by $xy\phi$,

$$v_{(AB)} = xv_{AA} + yv_{BB} + xy\phi(v_{AA} + v_{BB}). \qquad (16)$$

In terms of cell volume, equation (16) becomes

$$\phi = V_{exc}/n_{Ab}n_{Or}(V_{Ab} + V_{Or}), \qquad (17)$$

that is, ϕ is an excess volume, which is normalized depending on composition. This normalization makes ϕ a very sensitive measure of the variation of non-ideality with composition, as is seen from a consideration of equation (6). We have

$$V_{exc}/n_{Ab}n_{Or} = n_{Ab}W_{V(Or)} + n_{Or}W_{V(Ab)} \qquad (18)$$

when V_{exc} can be fitted by a third order polynomial, and

$$V_{exc}/n_{Ab}n_{Or} = W_V \qquad (19)$$

when a parabolic fit is appropriate ($W_{V(Ab)} = W_{V(Or)}$). Thus, if V_{exc} follows a third order curve, ϕ follows a straight line; if V_{exc} follows a parabola, ϕ is constant. Any deviation of V or V_{exc} from a second or third order curve, which may not be obvious from an inspection of a plot or even of the least-squares run, will clearly show up in the variation of ϕ.

In Figure 10 ϕ is plotted for the ordered and disordered alkali feldspar series. Curves were drawn through the data points using the polynomials of Table 10. Although ϕ is always positive, because V_{exc} is positive, it changes strongly with composition, that is, dilatation and contraction change their relative contribution to the excess volume.

In the LA–LM series ϕ is largest for Or-rich compositions, which is reasonable from a structural point of view. When in low microcline Na-atoms replace potassium they substitute on nine-coordinated sites such that the Na–O distances will be larger than in low albite, resulting in a positive excess volume and a large ϕ value. On the Na-rich side ϕ is close to zero, which may be attributed to a tendency to Na,K ordering in the sense of Iiyama (1974).

In the AA–HS series the shape and size of the Na,K-sites are influenced by the local Al,Si arrangement. Due to the random Al,Si distribution, those sites which due to their different sizes are favorable for occupation by either Na or K would also occur at random, which makes Na,K ordering in the high series less probable than in the low series. Thus ϕ is larger in analbite than in low albite, but still follows the same trend as in low albite. On the other hand, on the K-rich side ϕ is smaller in the high than in the low series. This again may be due to the random Al,Si distribution which in contrast to low microcline provides sites with CN < 9 which Na would enter preferentially. The question of Na,K ordering in AA–HS solutions was discussed from a thermodynamic point of view by Thompson and Hovis (1979) and Haselton et al. (1983).

The maximum value of ϕ is not found at the same composition as is the maximum excess volume. In contrast to $V_{exc(max)}$ ϕ_{max} marks those compositions in which contraction is absent or minimal. In the AA–HS series this occurs at $\sim Or_{35}$ where the displacive monoclinic/triclinic symmetry change is found. This coincidence is probably not fortituous; it is most likely related to the structural fluctuations that occur near the symmetry change.

Conclusion

The feldspar solid solution series presented in this paper were carefully prepared to ensure constant Al,Si distribution and complete homogenization across each series. In particular, the ordered and disordered alkali-feldspar series may serve as a reference for lattice parameters. Their volume behavior is interpreted in terms of two factors (v. Steinwehr, 1967): geometrical dilatation and chemical contraction. Their relative importance depends on the degree of Al,Si order. Geometrical dilatation, resulting in a positive excess volume, is thought to predominate in the AA–HS series, whereas chemical contraction attributed to Na,K ordering is suggested to decrease the excess volume near LA in the LA–LM series. Both series, especially LA–LM, show a definite deviation from symmetrical volume behavior resulting in Margules parameters $W_{v(Ab)} > W_{v(Or)} > 0$. Their difference increases with increasing Al,Si order.

Acknowledgments

The authors wish to thank Prof. H.-R. Wenk, Berkeley, California, who generously provided large quantities of Cazadero albite without which we could not have done our experiments. We also want to thank Prof. P. H. Ribbe, Blacksburg, Virginia, J. R. Goldsmith and J. V. Smith, Chicago, Illinois, for the time and labor they took in reviewing the manuscript.

References

Borg, I. Y. and Smith, D. K. (1969) Calculated powder patterns. Part II. Six potassium feldspars and barium feldspar. American Mineralogist, 54, 163–181.

Corlett, M. and Eberhard, E. (1967) Das Material für chemische und physikalische Untersuchungen an Plagioklasen. (Teil I der Laboratoriumsuntersuchungen an Plagioklasen.) Schweizerische Mineralogische und Petrographische Mitteilungen, 47, 303–316.

Goldsmith, J. R. and Laves, F. (1954) The microcline–sanidine stability relations. Geochimica et Cosmochimica Acta, 5, 1–19.

Harlow, G. E. (1982) The anorthoclase structures: the effects of temperature and composition. American Mineralogist, 67, 975–996.

Haselton, H. T., Jr., Hovis, G. L., Hemingway, B. S., and Robie, R. A. (1983) Calorimetric investigation of the excess entropy of mixing in analbite–sanidine solid solutions: lack of evidence for Na,K short-range order and implications for two-feldspar thermometry. American Mineralogist, 68, 398–413.

Hovis, G. L. (1977) Unit-cell dimensions and molar volumes for a sanidine–analbite ion-exchange series. American Mineralogist, 62, 672–679.

Hovis, G. L. (1980) Angular relations of alkali feldspar series and the triclinic–monoclinic displacive transformation. American Mineralogist, 65, 770–778.

Hovis, G. L. and Peckins, E. (1978) A new x-ray investigation of maximum microcline crystalline solutions. Contributions to Mineralogy and Petrology, 66, 345–349.

Iiyama, J. T. (1974) Substitution, déformation locale de la maille et équilibre de distribution des éléments en traces entre silicates et solution hydrothermale. Bulletin de la Société française de Minéralogie et de Cristallographie, 97, 143–151.

Johannes, W. (1979) Ternary feldspars: kinetics and possible equilibria at 800°C. Contributions to Mineralogy and Petrology, 68, 221–230.

Kroll, H. (1978) The structure of heat-treated plagioclases An_{28}, An_{52}, An_{69} and the estimation of Al,Si order from lattice parameters. (Abstr.) Physics and Chemistry of Minerals, 3, 76–77.

Kroll, H. (1983) Lattice parameters and determinative methods for plagioclase and ternary feldspars. In P. H. Ribbe, Ed., Feldspar Mineralogy, Reviews in Mineralogy, Vol. 2, 2nd ed., 101–119.

Kroll, H. (1984) Thermal expansion of alkali feldspars. In W. L. Brown, Ed., Feldspars and Feldspathoids, p. 163–205. Reidl, Dordrecht, Netherlands.

Kroll, H. and Bambauer, H.-U. (1981) Diffusive and displacive transformation in plagioclase and ternary feldspar series. American Mineralogist, 66, 763–769.

Kroll, H. and Ribbe, P. H. (1983) Lattice parameters, composition and Al,Si order in alkali feldspars. In P. H. Ribbe, Ed., Feldspar Mineralogy, Reviews in Mineralogy, Vol. 2, 2nd ed., 57–99.

Kroll, H., Baumbauer, H.-U., and Schirmer, U. (1980) The high albite–monalbite and analbite–monalbite transitions. American Mineralogist, 65, 1192–1211.

MacKenzie, W. S. (1954) The orthoclase–microcline inversion. Mineralogical Magazine, 30, 354–366.

Newton, R. C. and Wood, B. J. (1980) Volume behavior of silicate solid solutions. American Mineralogist, 65, 733–745.

Orville, P. M. (1967) Unit-cell parameters of the microcline–low albite and the sanidine–high albite solid solution series. American Mineralogist, 52, 55–86. Correction, 346–347.

Ribbe, P. H. (1983) Guides to indexing feldspar powder patterns. Feldspar Mineralogy, Reviews in Mineralogy, Vol. 2, 2nd ed., 325–341.

Salje, E., Kuscholke, B., Wruck, B., and Kroll, H. (1985) Thermodynamics of sodium feldspar II: Experimental results and numerical calculations. Physics and Chemistry of Minerals, 12, 99–107.

Smith, J. V. (1970) Physical properties of order–disorder structures with special reference to feldspar minerals. Lithos, 3, 145–160.

Smith, J. V. (1974) Feldspar Minerals. I. Crystal Structure and Physical Properties. Springer-Verlag, Heidelberg, 627 pp.

v. Steinwehr, H. E. (1967) Ursachen der Abweichungen von der Vegardschen Regel. Zeitschrift für Kristallographie, 125, 360–376.

Stewart, D. B. and Wright, T. L. (1974) Al/Si order and symmetry of natural alkali feldspars, and the relationship of strained cell parameters to bulk composition. Bulletin de la Société française de Minéralogie et de Cristallographie, 97, 356–377.

Strob, W. (1983) Strukturverfeinerung eines Tief-Mikroklins, Zusammenhänge zwischen ⟨T–O⟩ Abständen und Al,Si-Ordnungsgrad und metrische Variation in einer Tief-Albit/Tief-Mikroklin-Mischkristallreihe. Diplomarbeit, Inst. f. Mineralogie, Westf. Wilhelms-Universität, Münster.

Thompson, J. B., Jr. (1967) Thermodynamic properties of simple solutions. In P. H. Abelson, Ed., Researches in Geochemistry, II, p. 340–361. John Wiley and Sons, New York.

Thompson, J. B., Jr., Waldbaum, D. R., and Hovis, G. L. (1974) Thermodynamic properties related to ordering in end-member alkali feldspars. In W. S. MacKenzie and J. Zussman, Eds., The Feldspars, p. 218–248. Manchester University Press, Manchester.

Thompson, J. B., Jr. and Hovis, G. L. (1979) Entropy of mixing in sanidine. American Mineralogist, 64, 57–65.
Viswanathan, K. (1971) A new X-ray method to determine the anorthite content and structural state of plagioclases. Contributions to Mineralogy and Petrology, 30, 332–335.
Viswanathan, K. (1972) Kationenaustausch an Plagioklasen. Contributions to Mineralogy and Petrology, 37, 277–290.
Waldbaum, D. R. and Thompson, J. B., Jr. (1968) Mixing properties of sanidine crystalline solutions: II. Calculations based on volume data. American Mineralogist, 53, 2000–2017.
Waldbaum, D. R. and Robie, R. A. (1971) Calorimetric investigation of Na–K mixing and polymorphism in the alkali feldspars. Zeitschrift für Kristallographie, 134, 381–420.
Wenk, H.-R. and Kroll, H. (1984) Analysis of P$\bar{1}$, I$\bar{1}$ and C$\bar{1}$ plagioclase structures. Bulletin de Minéralogie, 107, 467–487.
Winter, J. K., Okamura, F. P., and Ghose, S. (1979) A high temperature structural study of high albite, monalbite, and the analbite–monalbite phase transition. American Mineralogist, 64, 409–423.
Wright, T. L. (1968) X-ray and optical study of alkali feldspar. II. An X-ray method of determining the composition and structural state from measurement of 2 values for three reflections. American Mineralogist, 53, 88–104.

Manuscript received, February 21, 1985;
accepted for publication, September 4, 1985.